J Math Chem (2011) 49:1291–1301
DOI 10.1007/s10910-011-9818-3

ORIGINAL PAPER

Finding minimum energy reaction paths on ab initio potential energy surfaces using the fast marching method

Yuli Liu · Paul W. Ayers

Received: 1 March 2011 / Accepted: 9 April 2011 / Published online: 29 April 2011

Abstract The fast marching method (FMM) for determining minimum-cost paths has been extended to compute the minimum-energy reaction coordinates in chemical reactions. This was accomplished by building an interface between FMM and the *Gaussian* program. We demonstrate the new method using an S_N2 reaction, the isomerization of HSCN to HNCS, and a gas-phase rearrangement reaction of relevance in mass spectrometry.

Keywords Fast-marching method · Minimum energy path · Intrinsic reaction coordinate · Reduced potential energy surface

1 Introduction

The multidimensional potential energy surface (PES) of a molecular system contains important information about the geometries and relative energies of its locally stable structures, as well as the reaction paths between them. When the reactants and products are known, the chemical reaction coordinate is often associated with the minimum energy path (MEP) connecting the reactant to the product. Once the MEP has been found, one knows the reaction mechanism, which is ordinarily characterized in terms of the local energy minima (reactive intermediates) and energy maxima (transition states) along the reaction path. One can also use the MEP to estimate the rate of reaction (using transition state theory).

Unfortunately, finding the minimum-energy reaction path is generally difficult. For simple reactions or reactions in which abundant experimental information is available beforehand, one can often make a "good guess" for the reaction path and then refine it

Y. Liu · P. W. Ayers (✉)
Department of Chemistry, McMaster University, 1280 Main St. West, Hamilton, ON, Canada
e-mail: ayers@mcmaster.ca

using a method like the nudged elastic band [1–4] or the quadratic string method [5–8]. In other cases, one can profitably use methods like coordinate driving [9], eigenvector-following techniques [10–13], or synchronous transit-guided Quasi-Newton [14,15] to locate the transition state; the ordinary intrinsic-reaction coordinate (IRC) algorithm [16–19] then suffices to find the minimum energy path. This approach, however, does not work for multi-step reaction mechanisms. While two-point methods like the quadratic string method are perfectly valid even for complex multi-step reaction mechanisms, finding a "good guess" for the reaction path becomes exponentially more difficult as the complexity of the reaction mechanism increases. We would like to have a more robust way to determine reaction paths for complex reaction mechanisms.

Recently, we have proposed adapting the fast-marching method (FMM) to determine minimum-energy reaction paths in complex multi-step reactions [20–25]. The fast-marching method is a numerical scheme for solving the nonlinear eikonal equation and related static Hamilton-Jacobi equations [26–29]. By defining an energy-cost function between the reactant and any other point, the fast marching method can transform the potential energy surface (PES) or free energy surface to an energy-cost surface. Unlike the multi-well PES, the energy-cost surface is a conical surface with a single minimum (the starting point, which is ordinarily either the reactant or the product of the chemical reaction). Moreover, given any molecular configuration, the minimum energy path is simply located by finding the steepest-descent path on the energy-cost surface. The process of finding this steepest-descent path is called backtracing.

In previous work, we applied the FMM method to some analytical two-dimensional potential energy surfaces [22]. Those results were quite favorable, so we elected to extend the method to higher-dimensional PES and interface the method with an electronic structure theory program, so that we could explore reactions for which analytical PES are unavailable. This paper reports our efforts in these directions. We have also worked on developing interpolation methods to reduce the number of quantum chemistry calculations that are needed to model the potential energy surface; those results have been reported separately [24,30]. Escobedo has also applied the fast-marching method to chemical dynamics, but his focus is primarily chemical waves in inhomogeneous reactive media, not reaction-pathway determination [31].

In the next section of this paper, we will briefly review the FMM methodology. Then we will present applications to three chemical reactions, of increasing complexity. We conclude with some comments on the extensions and improvements that we are currently pursuing.

2 The fast-marching method

We define the cost function at $\mathbf{R}$ as the "minimum cost" required to attain this configuration starting from configuration $\mathbf{R}_0$:

$$U_n(\mathbf{R}) = \underbrace{\min}_{\mathbf{C}_{\mathbf{R}_0,\mathbf{R}}(s)} \int_0^L \left\{\sqrt{2(E - V(\mathbf{C}(s)))}\right\}^n ds. \tag{1}$$

Here the minimization is over all paths, $\mathbf{C}_{\mathbf{R}_0,\mathbf{R}}(s)$, that start at $\mathbf{R}_0$ and end at $\mathbf{R}$, E is the total energy of the system, $V(\mathbf{R})$ is the potential energy surface, and L is the path length [22] (So $\mathbf{C}_{\mathbf{R}_0,\mathbf{R}}(0) = \mathbf{R}_0$ and $\mathbf{C}_{\mathbf{R}_0,\mathbf{R}}(L) = \mathbf{R}$). The path integral problem, (1), can be conveniently restated as an eikonal equation, namely,

$$|\nabla U_n(\mathbf{R})| = \left\{\sqrt{2(E - V(\mathbf{R}))}\right\}^n \tag{2}$$

The energy-cost of the reactant is zero by definition ($U(\mathbf{R}_0) = 0$); this is the boundary condition for the eikonal equation.

This eikonal equation describes wavefront propagation with the local speed function $\frac{1}{\{\sqrt{2(E-V(\mathbf{R}))}\}^n}$. To locate the MEP, we need the cost of molecular configurations with higher potential energy to be infinitely larger than the cost of configurations with lower potential energy (Equivalently, we need for configurations that are lower in energy to be attained infinitely faster than configurations that are higher in energy). This can be achieved by letting $n \to -\infty$, which ensures that higher energy paths in Eq. 1 are cut off from the set of paths ($C_{\mathbf{R}_0,\mathbf{R}}$), giving only the MEP. Of course, in computational implementations we will choose n to be a sizeable (but non-infinite) negative number. In practice, it seems that results are usually good as soon as n is less than minus ten.

Solving this eikonal equation transforms a multi-well potential energy surface, $V(\mathbf{R})$, into a conical energy-cost surface $U(\mathbf{R})$. Information about the fast-marching scheme for the 2-dimensional eikonal equation can be found in Refs. [22,23]. Our previous implementation required a complete PES scan in advance, which is very expensive and tends to fail at some regions (e.g., maxima on the PES). In order to apply the fast marching method to arbitrary dimensional PES of chemical reactions, we need two key innovations: first we need an improved upwind derivative formula so that we can solve the d-dimensional eikonal equation. Second we need to interface the fast-marching program with a quantum chemistry package (we are using *Gaussian 03*) so that the potential energy can be computed at molecular configurations of interest. The new FMM program doesn't compute the complete PES; instead it will push the advancing wavefront outward along the equipotential contours and call *Gaussian 03* to calculate the potentials of the points on the front. The energy-cost values are then computed by solving the eikonal Eq. 2.

We need to solve the eikonal equation using an upwind finite difference approximation, which will preserve the causality of the solutions. To do this, we discretize the eikonal equation as follows:

$$\left(\frac{(U-a_1)^+}{dR(1)}\right)^2 + \left(\frac{(U-a_2)^+}{dR(2)}\right)^2 + \cdots + \left(\frac{(U-a_d)^+}{dR(d)}\right)^2 = [2(E - V(\mathbf{R}))]^n \tag{3}$$

Here $dR(i)$ is the ith component of the grid size vector $d\mathbf{R}$; a_i is the smaller cost value of point $\mathbf{R}'s$ two neighbouring points in dimension i, $a_i = \min(U_{\text{left}}, U_{\text{right}})$, $(U-a_i)^+ = (U-a_i)$ if $U > a_i$ and $(U-a_i)^+ = 0$ otherwise (That is, $(U-a_i)^+ = \max(0, U-a_i)$). The "upwind finite difference," $(U-a_i)^+$, enforces the causality condition in the fast marching method, which means the cost can only increase while

the interface moves outward. In other words, for the point in question, its unknown cost value U has to be greater than the cost value, a_i, of its known neighbouring point; if $a_i > U$, then the cost value of this neighbouring point must not be known either. We can not use an unknown point, so we discard it by letting $(U - a_i)^+ = 0$. This is the idea behind the upwind finite difference approximation.

Equation 3 can be solved in an iterative way. First the $a_i's$ are sorted in increasing order. Start from $j = 1$ and solve the truncated equation:

$$\left(\frac{(U - a_1)^+}{dR(1)}\right)^2 = [2(E - V(\mathbf{R}))]^n \tag{4}$$

If the solution $U_1 \leq a_2$, then $U_1 \leq a_3 \leq \cdots \leq a_d$ and $U = U_1$ is also the solution to Eq. 3. If $U_1 > a_2$, then let $j = j + 1$, and continue to solve the truncated equation with 2 terms on the left side. This process is repeated until we find the jth solution $U_j \leq a_{j+1}$, $1 \leq j \leq d$.$U = U_j$ is the solution to Eq. 2.3 [29].

After computing the energy-cost values of all points on the interface, the heapsort technique is used to sort these values to find the point with minimum cost (thus the maximum local speed). The FMM program then accepts this point and calls *Gaussian 03* to compute the potentials at any neighboring points where the potential is unknown.

The FMM loop is then repeated, and the set of points for which the energy cost, U_j, is known systematically expands until the product is found.

Conceptually, we imagine slowly adding water to the reactant valley; the "water" level will keep going up, wetting the contours of the potential energy surface as it does so. Eventually the water level will rise to the level of the lowest-energy transition state, which is the lowest "mountain pass" for exiting the reactant valley. At this stage a narrow thread of water will follow the steepest-descent path to the bottom of the next valley. This process is mimicked by the FMM procedure. In FMM, the "energy cost" contours to record which portions of the potential energy surface are "flooded" at any given point in time.

Notice that only the "flooded" portion of the surface needs to be computed. This reduces the computational cost significantly. Moreover, the method is amenable to parallel computation: since the "beach" where the water meets the land expands in many directions at once, many different potential energy calculations can be performed simultaneously.

3 Applications

To demonstrate our revised and extended FMM program, we will give some examples using reduced 2-dimensional and 3-dimensional PES. Our FMM program is interfaced with *Gaussian 03* [32]. All *Gaussian* calculations were done using density-functional theory (BhandhLYP/6-311++G**) [33–37]. The "half and half" hybrid functional has less self-interaction error than the more popular hybrid functionals (like B3LYP). This is believed to be important for modeling the transition state structures where the exchange-correlation hole is delocalized [38–41] (The S_N2 reaction is a classic example of such a transition state).

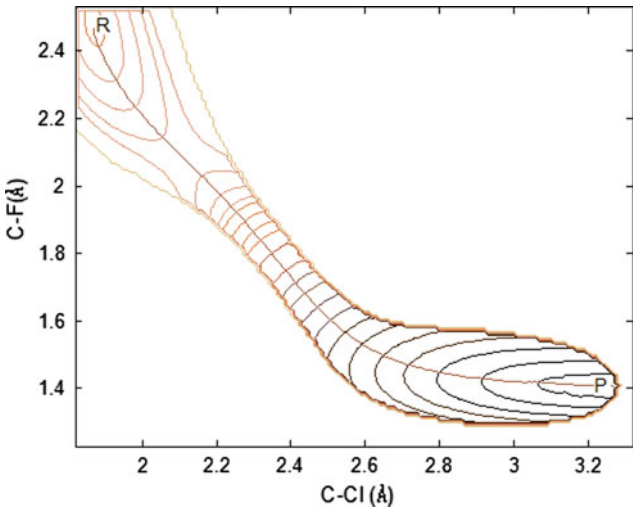

Fig. 1 The potential energy surface of the S_N2 reaction based on C–F and C–Cl bond lengths. The grid sizes on both dimensions are dR = 0.01 Å. The calculation starts from the reactant (R), fills the reactant valley, breaches the reaction barrier at the transition state (TS), and then "flows" down to the product (P). The FMM program transforms this PES to an energy-cost surface (Fig. 2)

3.1 The S_N2 reaction

The mechanism of the S_N2 reaction has been studied extensively by experimental and theoretical methods, so it is a good test for our method. This is a one-step reaction, so we expect two minima (the reactant R and product P) and one transition state (TS) on the PES.

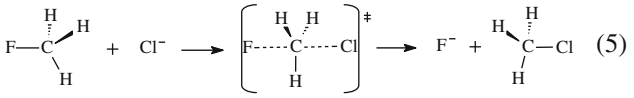

(5)

In this reaction, only C–F and C–Cl bonds are involved in bond-breaking and bond-forming, so the PES of this reaction can be modelled using a 2-dimensional reduced potential energy surface based on the C–F and C–Cl coordinates [42]. At each grid point, we will freeze the C–F and C–Cl bond length at the given values and minimize the energy with respect to the other coordinates. The 2-dimensional reduced PES and the MEP computed by the FMM program are depicted in Fig. 1. About 20% of grid points are in the "flooded" region and are computed by *Gaussian 03*. The energy-cost surface with the reactant (R) as starting point and the MEP found on this surface are shown in Fig. 2. Plotting the change in potential energy along the MEP gives the energy profile of the reaction coordinate (Fig. 3).

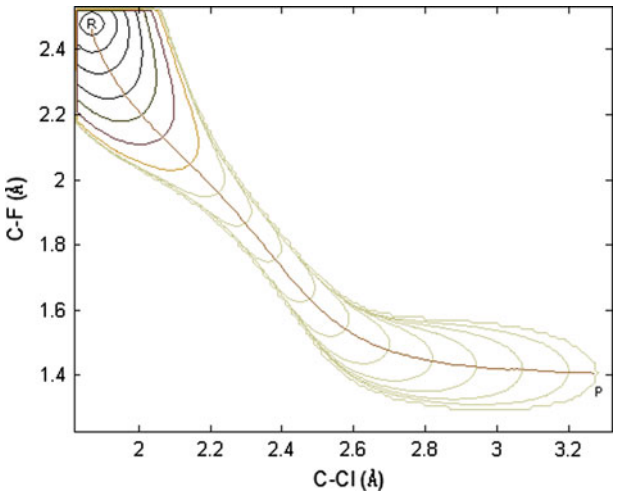

Fig. 2 The energy-cost surface transformed from the PES on Fig. 1. The MEP is determined by backtracing from the product to the reactant along the steepest descent path on the energy-cost surface

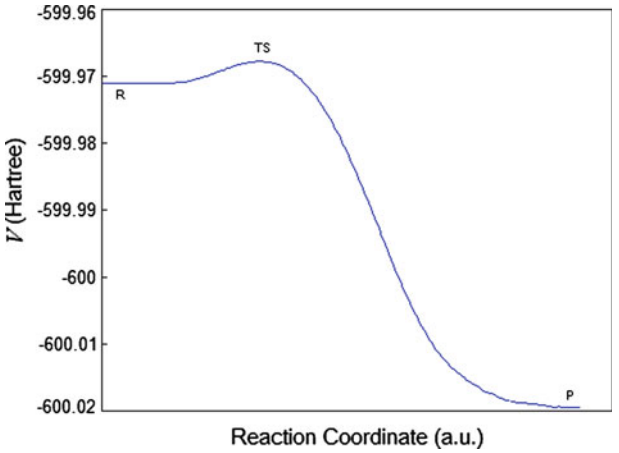

Fig. 3 The energy profile of the S_N2 reaction 8

3.2 The isomerization of HSCN to HNCS

Wierzejewska and Moc reported 9 isomers of HSCN [43]. For the isomerization reaction of HSCN to HNCS, they proposed two competitive mechanisms. The first one is a one-step mechanism,

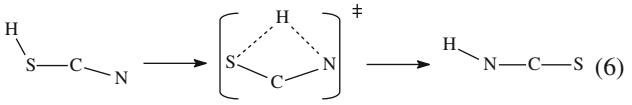

(6)

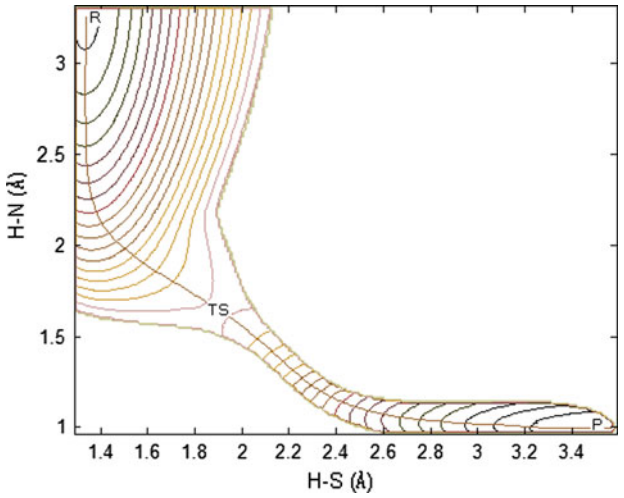

Fig. 4 The reduced 2-dimensional PES for the isomerization of HSCN to HNCS, based on H–S and H–N bond lengths

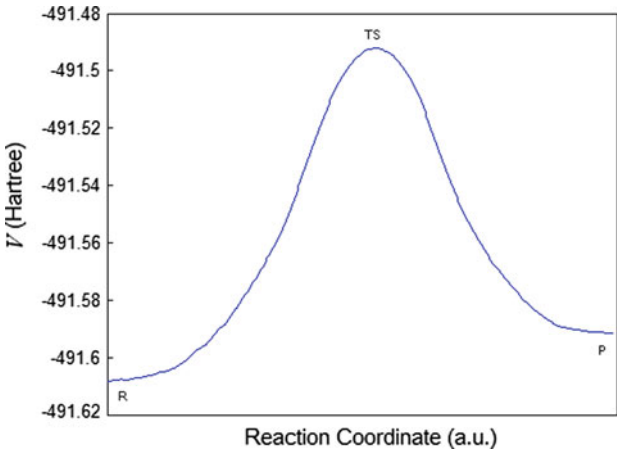

Fig. 5 The energy profile for the isomerization of HSCN to HNCS

The second mechanism is a two-step mechanism with a ring structure intermediate,

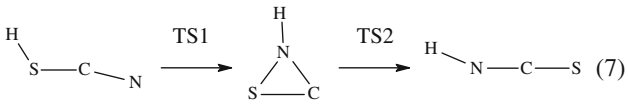

(7)

According to Wierzejewska and Moc [43] the first mechanism has the lower energy barrier. We will test this conclusion using the FMM program. The H–S and H–N bond lengths are chosen as the key coordinates. Figure 4 shows the reduced 2-dimensional PES based on these two key coordinates and the MEP found on the energy-cost sur-

face. The results are similar to those from previous studies, but the FMM program only computes about 30% of the grid points.

The energy profile of the reaction coordinate is shown in Fig. 5.

3.3 The dissociation of ionized O-methylhydroxylamine

One strength of the FMM approach is that it can be applied to any number of dimensions. The cost, of course, will grow exponentially with increasing dimensionality because of the increasing number of stationary points on the potential energy surface, and the results become increasing difficult to visualize as dimensionality increases [44]. As a simple example that is neither too expensive nor too difficult to visualize, we consider the dissociation of $[CH_5NO]^{+\bullet}$.

The PES of $[CH_5NO]^{+\bullet}$ has been studied using mass spectrometry and theoretical methods [45]. The following dissociation reaction has been observed,

$$[CH_5NO]^{+\bullet} \rightarrow [CH_2NH_2]^{+} + OH^{\bullet} \tag{8}$$

and the mechanism proposed for this dissociation reaction is [45]

$$CH_3{-}O{-}NH_2^{+\bullet} \rightarrow \overset{\bullet}{O}{-}\overset{+}{N}H_2{-}CH_3 \rightarrow H\overset{\bullet}{O}{-}NH_2 - \overset{+}{C}H_2 \rightarrow H\overset{\bullet}{O} + NH_2\overset{+}{C}H_2 \tag{9}$$

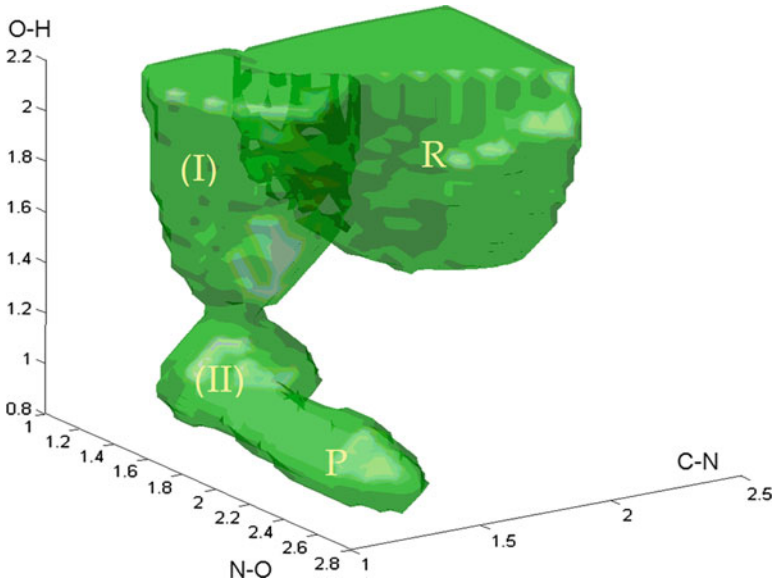

Fig. 6 The isosurface with a potential value of −170.534 Hartrees, which is one layer of the reduced 3-dimensional PES for the dissociation reaction of ionized O-methylhydroxylamine. The 3-dimensional equi-potential surfaces have an onion-like structure. Each layer of the "onion" represents a certain value of the potential energy. The cores of the "onions" are minima on the PES

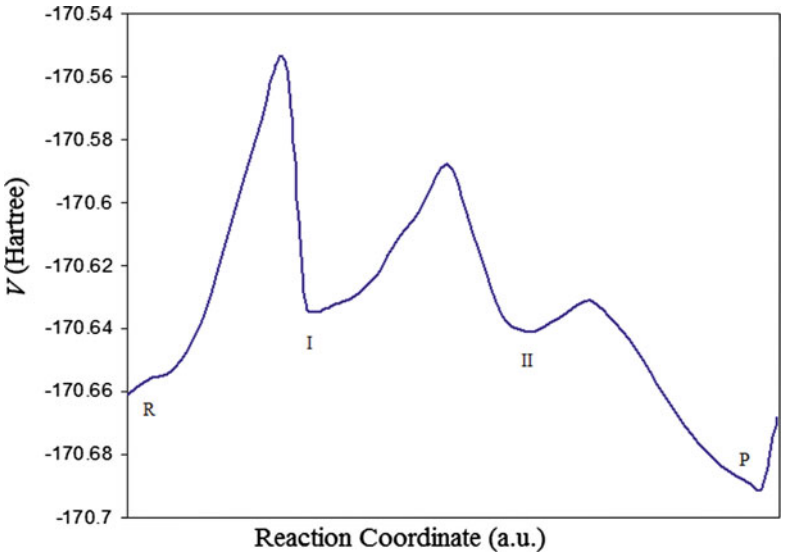

Fig. 7 The energy profile of the dissociation reaction of ionized O-methylhydroxylamine

We selected the bond lengths C–N, N–O and O–H as the key coordinates, then performed FMM on the 3-dimensional reduced PES defined by these points. The 3-dimensional equi-potential surfaces have onion-like structures. Each layer of the "onion" represents a certain value of the potential energy. Figure 6 shows one layer of the "onion" with a potential value of −170.534 Hartrees. The cores of onions represent minima on the PES. We can see that there are 4 minima on this PES, the reactant (R), two intermediates (I, II), and the product (P). By examining the structures obtained, we deduce that intermediate (I) and (II) coincide with $\dot{\mathrm{O}}-\overset{+}{\mathrm{N}}\mathrm{H}_2-\mathrm{CH}_3$ and $\mathrm{H}\dot{\mathrm{O}}-\mathrm{NH}_2-\overset{+}{\mathrm{C}}\mathrm{H}_2$, respectively. The FMM calculation confirms that the mechanism in (9) is the minimum energy reaction pathway.

Figure 7 shows the energy profile along the dissociation pathway in Rxn (9). This sort of several-step reaction is very difficult for most reaction-path methods, but FMM works just as well for this reaction as it does for the much simpler isomerization of HSCN.

4 Conclusion

The fast marching method (FMM) is a very general method for finding the minimum energy path (MEP). Without any information about the mechanism in advance, it can find the minimum energy reaction path linking the reactant and any other point on the potential energy surface (PES). Due to its reliable and unbiased nature, the fast marching method can find the minimum energy path for any kind of chemical reactions. However, the computation cost of FMM is relatively high because a significant portion of the potential energy surface has to be computed in order to rigorously determine the MEP. This is especially true for 3 or higher dimensional PES.

The computation of points on the potential energy surface is several orders of magnitude more costly than solving the eikonal equation or performing the heap sort. Thus, before we make routine applications to higher-dimensional PES and more complicated molecules, we need to reduce the number of potential-energy computations that are required. Using a combination of moving-least-squares [46–50] and Shepard interpolation [51,52] reduces the number of potential energy computations that are required [24]. We can also reduce the cost of this method by performing potential energy computations all along the expanding front concurrently, with each point on the expanding front assigned to a different processor, and/or by parallelizing the constrained geometry optimizations that are needed to construct the reduced potential energy surfaces [53]. It is also useful to run the fast-marching method on a relatively course grid, and then refine the estimates of the geometries and energies of the transition states using conventional methods (One such method, recently developed in our group, exploits the same "reduced potential energy" structure as the underlying FMM approach [54]). Finally, in cases where the full reaction path is not needed, and it suffices to only characterize the preferred mechanism and the transition state of the rate-limiting step, dual grid methods like the boundary-low-path method may be preferred [30].

Acknowledgments The authors thank the chemistry department of McMaster University, the Mutual Group graduate scholarship of McMaster University, NSERC, Sharcnet, and the Canada Research Chairs for research support.

References

1. G. Mills, H. Jonsson, Phys. Rev. Lett. **72**, 1124 (1994)
2. G. Henkelman, H. Jonsson, J. Chem. Phys. **113**, 9978 (2000)
3. G. Henkelman, B.P. Uberuaga, H. Jonsson, J. Chem. Phys. **113**, 9901 (2000)
4. B. Peters, A. Heyden, A.T. Bell, A. Chakraborty, J. Chem. Phys. **120**, 7877 (2004)
5. S.K. Burger, W.T. Yang, J. Chem. Phys. **124**, 224102 (2006)
6. S.K. Burger, W.T. Yang, Chem. J. Phys. **124**, 054109 (2006)
7. W.N.E.W.Q. Ren, E. Vanden-Eijnden, Phys. Rev. B **66**, 052301 (2002)
8. W.N.E.W.Q. Ren, E. Vanden-Eijnden, J. Chem. Phys. **126**, 164103 (2007)
9. I. Berente, G. Naray-Szabo, J. Phys. Chem. A **110**, 772 (2006)
10. J. Nichols, H. Taylor, P. Schmidt, J. Simons, J. Chem. Phys. **92**, 340 (1990)
11. J. Simons, P. Jorgensen, H. Taylor, J. Ozment, J. Phys. Chem. **87**, 2745 (1983)
12. A. Banerjee, N. Adams, J. Simons, R. Shepard, J. Phys. Chem. **89**, 52 (1985)
13. G. Henkelman, H. Jonsson, J. Chem. Phys. **111**(15), 7010 (1999)
14. C.Y. Peng, H.B. Schlegel, Isr. J. Chem. **33**, 449 (1993)
15. C.Y. Peng, P.Y. Ayala, H.B. Schlegel, M.J. Frisch, J. Comput. Chem. **17**, 49 (1996)
16. K. Fukui, Acc. Chem. Res. **14**(12), 363 (1981)
17. C. Gonzalez, H.B. Schlegel, J. Chem. Phys. **90**, 2154 (1989)
18. C. Gonzalez, H.B. Schlegel, J. Phys. Chem. **94**, 5523 (1990)
19. S.K. Burger, W.T. Yang, J. Chem. Phys. **125**, 244108 (2006)
20. B.K. Dey, S. Bothwell, P.W. Ayers, J. Math. Chem. **41**, 1 (2007)
21. B.K. Dey, P.W. Ayers, Mol. Phys. **105**, 71 (2007)
22. B.K. Dey, P.W. Ayers, Mol. Phys. **104**, 541 (2006)
23. B.K. Dey, M.K. Janicki, P.W. Ayers, J. Chem. Phys. **121**, 6667 (2004)
24. S.K. Burger, Y.L. Liu, U. Sarkar, P.W. Ayers, J. Chem. Phys. **130**, 024103 (2009)
25. Y.L. Liu, S.K. Burger, B.K. Dey, U. Sarkar, M. Janicki, P.W. Ayers, in *Quantum Biochemistry*, ed. by C.F. Matta (Wiley-VCH, Boston, 2010)
26. J.A. Sethian, A. Vladimirsky, Siam J. Numer. Anal. **41**(1), 325 (2003)

27. J.A. Sethian, SIAM Rev. **41**(2), 199 (1999)
28. J.A. Sethian, Proc. Natl. Acad. Sci. **93**(4), 1591 (1996)
29. H.K. Zhao, Math. Comput. **74**(250), 603 (2005)
30. S.K. Burger, P.W. Ayers, J. Chem. Theory Comput. **6**, 1490 (2010)
31. R. Escobedo, Int. J. Quantum Chem. **108**, 848 (2008)
32. M.J. Frisch, G.W. Trucks, H.B. Schlegel, G.E. Scuseria, M.A. Robb, J.R. Cheeseman, J.A. Montgomery, T. Vreven, K.N. Kudin, J.C. Burant, J.M. Millam, S.S. Iyengar, J. Tomasi, V. Barone, B. Mennucci, M. Cossi, G. Scalmani, N. Rega, G.A. Peersson, H. Nakatsuji, M. Hada, M. Ehara, K. Toyota, R. Fukuda, J. Hasegawa, M. Ishida, T. Nakajima, Y. Honda, O. Kitao, H. Nakai, M. Klene, X. Li, J.E. Knox, H.P. Hratchian, J.B. Cross, C. Adamo, J. Jaramillo, R. Gomperts, R.E. Stratmann, O. Yazyev, A.J. Austin, R. Cammi, C. Pomelli, J.W. Ochterski, P.Y. Ayala, K. Morokuma, G.A. Voth, O. Salvetti, J.J. Dannenberg, V.G. Zakrzewski, S. Dapprich, A.D. Daniels, M.C. Strain, O. Farkas, D.K. Malick, A.D. Rabuck, K. Raghavachari, J.B. Foresman, J.V. Ortiz, Q. Cui, A.G. Baboul, S. Clifford, J. Cioslowski, B.B. Stefanov, G. Liu, A. Liashenko, P. Piskorz, I. Komaromi, R.L. Martin, D.J. Fox, T. Keith, M.A. Al-Laham, C.Y. Peng, A. Nanayakkara, M. Challacombe, P.M.W. Gill, B. Johnson, W. Chen, M.W. Wong, C. Gonzalez, J.A. Pople, *Gaussian03, Revision C.02*. (Gaussian Inc., Wallingford, CT, 2004)
33. A.D. Becke, Phys. Rev. A **38**, 3098 (1988)
34. A.D. Becke, J. Chem. Phys. **98**, 5648 (1993)
35. A.D. Becke, J. Chem. Phys. **98**, 1372 (1993)
36. B. Miehlich, A. Savin, H. Stoll, H. Preuss, Chem. Phys. Lett. **157**(3), 200 (1989)
37. C. Lee, W. Yang, R.G. Parr, Phys. Rev. B **37**, 785 (1988)
38. P.W. Ayers, W. Yang, in *Computational Medicinal Chemistry for Drug Discovery*, ed. by P. Bultinck, H. de Winter, W. Langenaeker, J.P. Tollenaere (Dekker, New York, 2003), p. 571
39. O.V. Gritsenko, B. Ensing, P.R.T. Schipper, E.J. Baerends, J. Phys. Chem. A **104**, 8558 (2000)
40. Y. Zhang, W. Yang, J. Chem. Phys. **109**, 2604 (1998)
41. A.J. Cohen, P. Mori-Sanchez, W.T. Yang, Science **321**, 792 (2008)
42. P.W. Ayers, R.G. Parr, J. Am. Chem. Soc. **123**, 2007 (2001)
43. M. Wierzejewska, J. Moc, J. Phys. Chem. A **107**, 11209 (2003)
44. F.H. Stillinger, T.A. Weber, Science **225**(4666), 983 (1984)
45. P.C. Burgers, C. Lifshitz, P.J.A. Ruttink, G. Schaftenaar, J.K. Terlouw, Org. Mass Spectrom. **24**(8), 579 (1989)
46. T. Ishida, G.C. Schatz, J. Comput. Chem. **24**(9), 1077 (2003)
47. T. Ishida, G.C. Schatz, Chem. Phys. Lett. **314**(3-4), 369 (1999)
48. G.G. Maisuradze, D.L. Thompson, J. Phys. Chem. A **107**, 7118 (2003)
49. G.G. Maisuradze, D.L. Thompson, A.F. Wagner, M. Minkoff, J. Chem. Phys. **119**, 10002 (2003)
50. G.G. Maisuradze, A. Kawano, D.L. Thompson, A.F. Wagner, M. Minkoff, J. Chem. Phys. **121**, 10329 (2004)
51. D.L. Crittenden, M.J.T. Jordan, J. Chem. Phys. **122**(4), (2005)
52. M.A. Collins, Theor. Chem. Acc. **108**, 313 (2002)
53. S.K. Burger, P.W. Ayers, J. Chem. Phys. **133**, 034116 (2010)
54. S.K. Burger, P.W. Ayers, J. Chem. Phys. **132**, 234110 (2010)